Lipophilicity and click reactivity determine the performance of bioorthogonal tetrazine tools in pretargeted *in vivo* chemistry

E. Johanna L. Stéen[†,¥,Ŧ], Jesper T. Jørgensen[‡¥,Ŧ], Christoph Denk[¶,Ŧ], Umberto M. Battisti[†], Kamilla Nørregard[‡¥], Patricia E. Edem[†,‡], Klas Bratteby[¥,†,#], Vladimir Shalgunov[†,‡], Martin Wilkovitsch[¶], Dennis Svatunek[¶], Christian B. M. Poulie[†,‡], Lars Hvass[‡¥], Marina Simón[‡¥,Ŧ], Thomas Wanek[§], Raffaella Rossin[ǁ], Marc Robillard[ǁ], Jesper L. Kristensen[†], Hannes Mikula[¶,]*, Andreas Kjaer[‡,¥,]* and Matthias M. Herth[†,¥,]*

[†]Department of Drug Design and Pharmacology, Faculty of Health and Medical Sciences, University of Copenhagen, Universitetsparken 2, 2100 Copenhagen, Denmark.

[¥]Department of Clinical Physiology, Nuclear Medicine & PET, Rigshospitalet, Blegdamsvej 9, 2100 Copenhagen, Denmark.

[‡]Cluster for Molecular Imaging, Department of Biomedical Sciences, University of Copenhagen, Blegdamsvej 3, 2100 Copenhagen Ø, Denmark.

[#] Department of Radiation Physics, Skåne University Hospital, Barngatan 3, 22242 Lund, Sweden

[§§]Preclinical Molecular Imaging, AIT Austrian Institute of Technology GmbH, 2444 Seibersdorf, Austria

[¶]Institute of Applied Synthetic Chemistry, Technische Universität Wien (TU Wien), Getreidemarkt 9, 1060 Vienna, Austria.

[ǁ]Tagworks Pharmaceuticals, Geert Grooteplein 10, 6525 GA Nijmegen, Netherlands.

ABSTRACT

The development of highly selective and fast biocompatible reactions for ligation and cleavage has paved the way for new diagnostic and therapeutic applications of *in vivo* chemistry. The concept of bioorthogonal pretargeting has attracted considerable interest, in particular for the targeted delivery of radionuclides and drugs. In nuclear medicine, pretargeting can provide increased target-to-background ratios at early time-points compared to traditional approaches. This reduces the radiation burden to healthy tissue and, depending on the selected radionuclide, enables better imaging contrast or higher therapeutic efficiency. Moreover, bioorthogonally triggered cleavage of pretargeted antibody-drug conjugates represents an emerging strategy to achieve controlled release and locally increased drug concentrations. The toolbox of bioorthogonal reactions has significantly expanded in the past decade, with the tetrazine ligation being the fastest and one of the most versatile *in vivo* chemistries. Progress in the field, however, relies heavily on the development and evaluation of (radio)labeled compounds, preventing the use of compound libraries for systematic studies. The rational design of tetrazine probes and triggers has thus been impeded by the limited understanding of the impact of structural parameters on the *in vivo* ligation performance. In this work, we describe the development of a pretargeted blocking assay that allows for the investigation of the *in vivo* fate of a structurally diverse library of 45 unlabeled tetrazines and their capability to reach and react with pretargeted *trans*-cyclooctene (TCO)-tagged antibodies in tumor-bearing mice. This study enabled us to assess the correlation of click reactivity and lipophilicity of tetrazines with their *in vivo* performance. In particular,

high rate constants ($>50,000$ M^{-1}s^{-1}) for the reaction with TCO and low calculated log$D_{7.4}$ values (below -3) of the tetrazine were identified as strong indicators for successful pretargeted *in vivo* click chemistry. Click-radiolabeling gave access to a set of selected ^{18}F-labeled tetrazines, including highly reactive scaffolds, which were used in pretargeted PET imaging studies to confirm the results from the blocking study. These insights thus enable the rational design of tetrazine probes for *in vivo* application and will thereby assist the clinical translation of bioorthogonal pretargeting.

Keywords: bioorthogonal chemistry, tetrazine ligation, pretargeted imaging, PET, fluorine-18, molecular imaging

INTRODUCTION

The concept of *in vivo* chemistry based on the development of bioorthogonal reactions has led to a renaissance of pretargeting strategies in nuclear medicine and for controlled drug delivery.[1-4] Monoclonal antibodies (mAbs) have found wide-spread application in this regard, particularly as selective targeting vectors for specific antigens expressed on cancer cells.[5] For example, immuno-positron emission tomography (PET) can be used for precision medicine, *i.e.*, to guide the selection of patients, who show the highest probability to benefit from a specific therapy.[6,7] Similarly, radioimmunotherapy (RIT) is based on the application of the unique targeting ability of mAbs to deliver therapeutic radionuclides to diseased tissue, most often to tumors.[8] RIT has several advantages over conventional external radiation therapy, notably the ability to target and treat the entire tumor burden, including micrometastases.[8] However, due to the long blood circulation time of mAbs (several days to weeks), adequate tumor-to-background ratios are usually not achieved until 2–4 days after administration, requiring the use of long-lived radionuclides. Most often, this results in a relatively high radiation burden to the patient.[9,10] In order to reduce the absorbed radiation dose and reach higher tumor-to-background ratios at earlier time points, pretargeting has emerged as an efficient strategy, enabling *in vivo* radiolabeling of mAbs upon accumulation at their target.[2,10-16] This is realized by modifying the mAb with a specific reactive molecular tag, which can later selectively react with a radiolabeled agent via a rapid bioorthogonal reaction. Similarly, pretargeting can be applied for spatiotemporally controlled drug delivery. [2,17-21] In this approach, a highly potent drug is bioorthogonally cleaved from a pretargeted mAb-conjugate upon its accumulation at the site of disease, achieving higher local drug concentrations while simultaneously reducing systemic toxicity to healthy tissue. Due to its

fast reaction kinetics, high selectivity and biocompatibility, the inverse electron demand Diels-Alder (IEDDA)-initiated ligation between a 1,2,4,5-tetrazine (Tz) and a *trans*-cyclooctene (TCO) has become state-of-the-art for time-critical application of *in vivo* chemistry, as well as bioorthogonally controlled drug delivery by using Tz-triggered elimination of cleavable TCOs ('click-to-release'). [2,13,19-24] Currently, the understanding of the scope and limitations of IEDDA-initiated ligation for pretargeting strategies *in vivo* is limited and the design of suitable Tz-derivatives for this purpose is mainly a 'trial-and-error' game, heavily depending on the time-intensive development of radiolabeled compounds for *in vivo* evaluation. Current labeling strategies have, so far, mostly been focused on chelator approaches, overall impeding the use of compound libraries for systematic studies. [14,25,26] In order to enable the rational design of tetrazine derivatives for *in vivo* chemistry, it is important to understand the structure-property relationship between the physicochemical parameters of Tz-derivatives and their capability to reach and react *in vivo* with TCO-modified (bio)molecules accumulated at the target site of interest.

The aim of the present study was to identify and explore the key parameters that influence the *in vivo* performance of Tz-derivatives (Figure 1). Consequently, we prepared a library of Tz-derivatives with a set of different rate constants (in the reaction with TCO), lipophilicities, and topological polar surface areas (TPSA), and applied a pretargeted blocking assay to evaluate their ligation performance *in vivo*. The blocking effect of each Tz was correlated with its lipophilicity (calculated $\log D_{7.4}$ ($c\log D_{7.4}$) values), calculated TPSA as well as with its IEDDA reactivity. The obtained results were verified by *in vivo* pretargeted PET imaging of a set of selected Tz-derivatives radiolabeled with fluorine-18.
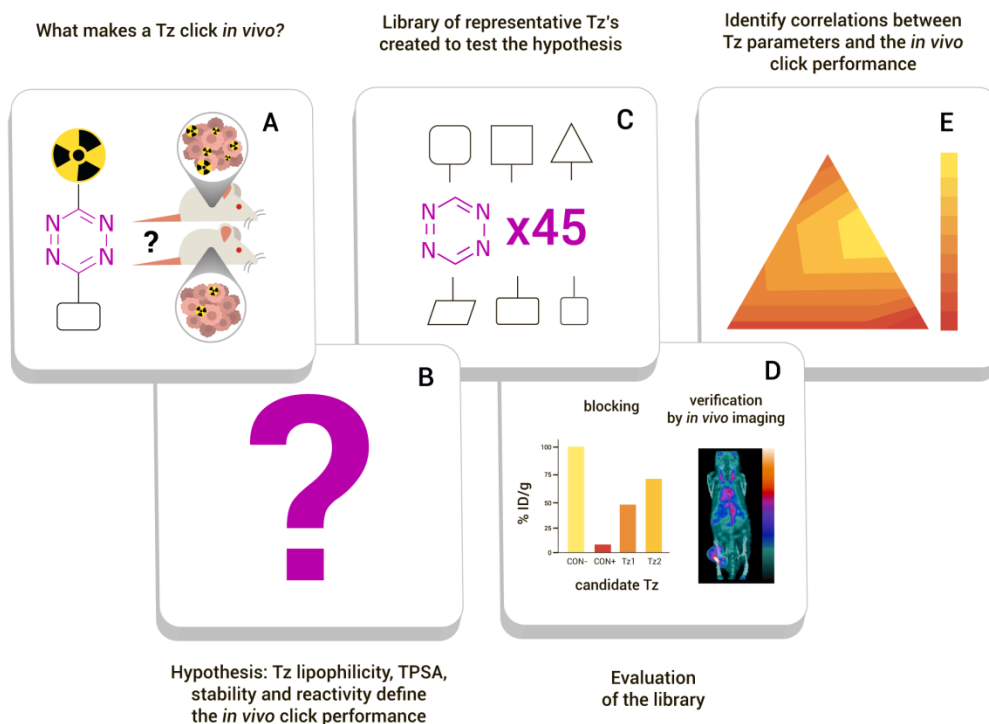
Figure 1. General strategy and workflow of this study. (**A**) The research question: Which key parameters determine the efficiency of the *in vivo* performance of tetrazines? (**B**) We hypothesized that lipophilicity, TPSA, stability and/or reactivity of the Tz determine its *in vivo* ligation efficiency. (**C**) To test this hypothesis, a compound library was created and (**D**) evaluated with emphasis on the capability for *in vivo* click reaction. (**E**) Finally, these results were analyzed to identify and confirm the correlation between key parameters and *in vivo* ligation performance.

RESULTS AND DISCUSSION

Experimental design and preparation of the Tz-library

A structurally diverse library of 45 Tz-derivatives was prepared, covering a wide spectrum of physicochemical properties, in particular calculated TPSAs between 60–350 Å^2 and different lipophilicities, with calculated log$D_{7.4}$ values (clog$D_{7.4}$) ranging from approximately -7.0 to 2.5 (Table 1; for synthetic procedures and details see Supporting Information). The Tz-scaffolds (A–L) include mono- and disubstituted methyl-, phenyl-, 2-pyrimidyl-, and 2-pyridyl-substituted Tz-derivatives with second-order rate constants for the reaction with TCO ranging from 1.4 to 230 M^{-1} s^{-1} in 1,4-dioxane at 25 °C, and from 1,100 to 73,000 M^{-1} s^{-1} in buffered aqueous solution at 37 °C. Table 1 provides an overview of the synthesized Tz-library and displays the measured rate constants and calculated physicochemical properties of each Tz. Several compounds were obtained as copper(II) complexes (for details see the Supporting Information), which was taken into account in the calculation of clog$D_{7.4}$ and TPSA (as described in the Notes of Table 1).

Table 1. Structural scaffolds, calculated physicochemical properties (TPSA and clog$D_{7.4}$), measured second-order rate constants for the ligation with TCO, and blocking efficiencies of all investigated Tz-derivatives.

Tz-scaffolds A, B, C, D, E, F, G, H, I, K, L

Ligands: DOTA, NOTA, PCB-TE$_2$A, NODAGA, DBCO

Tz	Tz-scaffold	R	clog$D_{7.4}$[a]	TPSA[a] (Å^2)	Rate constant (1,4-dioxane, 25 °C, M^{-1} s^{-1})[b]	Rate constant (DPBS, 37 °C, M^{-1} s^{-1})[b]	Blocking effect (%)[c]	% Tumor Uptake of [^{111}In]46 after blocking
1	A	(F-alkyl)	0.29	91	72	39,000	9	91
2	A	(F-PEG3)	-0.06	119	72	39,000	4	96
3	A	(F-sugar)	-1.53	161	72	39,000	80	20
4	A	(DOTA)	-2.86	217	72	39,000	95	5
5	B	(F-alkyl)	0.89	91	1.4	1,100	9	91
6	B	(F-PEG3)	0.54	119	1.4	1,100	1	99
7	B	(F-sugar)	-0.93	161	1.4	1,100	13	87
8	B	(DOTA)	-5.81	221	1.4	1,100	49	51
9	C	(NH$_2$)	-2.19	114	1.4	1,100	14	86
10	C	(DOTA)	-2.05	214	1.4	1,100	32	68
11	C	(PCB-TE2A)	-3.2	184	1.4	1,100	34	66
12	D	(F-alkyl)	1.89	104	13	n.d.	0	100
13	D	(F-PEG3)	1.53	132	13	n.d.	0	100
14	D	(F-sugar)	0.06	174	13	n.d.	24	76
15	D	(OH-acid)	-1.98	111	13	n.d.	78	22
16	D	(N(CH$_2$COOH)$_2$)	-6.65	167	13	n.d.	79	21
17	E	(F-alkyl)	0.65	82	200	60,000	0	100
18	E	(F-PEG3)	0.29	109	200	60,000	28	72
19	E	(F-sugar)	-1.18	152	200	60,000	76	24
20	E	(DOTA)	-2.46	208	200	60,000	94	6
21	F	-OH	-1.97	114	83	n.d.	87	13
22	F	(F-PEG3)	0.64	134	83	n.d.	27	73
23	F	(OH)	0.12	126	83	n.d.	72	28
24	F	(NODAGA)	-4.2	278	83	n.d.	96	4
25	G	(F-alkyl)	2.46	137	230	73,000	16	84
26	G	(F-PEG3)	2.10	164	230	73,000	30	70
27	G	(F-sugar)	0.63	207	230	73,000	51	49
28	H	(Boc)	1.11	90	210	58,000	45	55
29	H	(F-amide)	-0.14	78	210	58,000	55	45
30	H	(F-amine)	-0.18	63	210	58,000	62	38

No.		Structure						
31	H	$-NHC(O)CH_3$	-0.41	80	210	58,000	60	40
32	H	$-NHCH_2C(O)OH$	-3.03	100	210	58,000	86	14
33	H	-N(CH₂COOH)₂	-6.89	129	210	58,000	97	3
34	H	glutaramide-PEG₇-NH₂	-4.4	202	210	58,000	95	5
35	H	glutaramide-PEG₇-NOTA	-5.16	320	210	58,000	96	4
36	I	-	1.79	61	10	n.d.	0	100
37	K	$-NH_2$ chain	-0.77	129	230	73,000	76	24
38	K	amide-ethyl-NH₂	-2.23	161	230	73,000	83	17
39	K	$-C(O)OH$	-2.37	143	230	73,000	96	4
40	K	amide-PEG₁₁-NH₂	-3.81	263	230	73,000	97	3
41	K	amide-PEG₁₁-DOTA	-4.13	362	230	73,000	99	1
42	K	amide-PEG₆-amide-DBCO	1.62	129	230	73,000	75	25
43	L	$-CH_2CH_2F$	0.84	137	230	73,000	67	33
44	L	PEG₃-F	0.48	164	230	73,000	72	28
45	L	fluorosugar	-0.99	207	230	73,000	99	1

Notes: [a]The distribution coefficient at physiological pH ($\log D_{7.4}$) and TPSA were calculated using the software Chemicalize. Tetrazines conjugated to DOTA were calculated with chelated trivalent cations, Tzs with other chelators with bivalent cations. [b]Second-order rate constants for the Tz scaffolds A-L were determined by stopped-flow spectrophotometry ($n \geq 4$), monitoring the reaction of representative tetrazines with unsubstituted *trans*-cyclooctene (TCO) at 25 °C in 1,4-dioxane, and with TCO-PEG₄ (modified TCO-5*ax*-OH, '*minor-TCO*') in Dulbecco's phosphate buffered saline (DBPS) at 37 °C. [c]$n \geq 3$; (see Supporting Information, Table S1 and Table S2).

Pretargeted blocking studies

The blocking assay allows for the assessment of the *in vivo* ligation performance of unlabeled Tz-derivatives, avoiding the need for time-consuming development of radiolabeling procedures, as well as the preparation of labeled analogs or surrogates. The assay was inspired by receptor blocking experiments and based on the pretargeted imaging approach reported by Rossin *et al.*.[13,27] An ¹¹¹In-labeled Tz ([¹¹¹In]**46**, see Supporting Information, Fig. S1) was used in pair with TCO-modified CC49, a non-internalizing mAb that targets the tumor-associated glycoprotein 72 (TAG72),[13,27] as a benchmark model for the *in vivo* ligation. To study the *in vivo* ligation performance of Tz-derivatives **1**–**45**, BALB/c mice bearing LS174T colon carcinoma xenografts were injected intravenously (*i.v.*) with CC49-TCO 72 h prior to *i.v.* injection of the unlabeled Tz, followed by administration of [¹¹¹In]**46** 1 h later (for experimental details see Supporting Information). The animals were euthanized after 22 h and an *ex vivo* biodistribution was carried out to quantify the tumor uptake of [¹¹¹In]**46** (Figure 2A). The efficiency of the *in vivo* ligation of the unlabeled Tz can thus be correlated to a reduced uptake of [¹¹¹In]**46** (Fig. 2A). As a control, blocking was performed using the non-radioactive precursor of [¹¹¹In]**46** (DOTA-Tz **41**, see Supporting Information), which blocked ≥99% of the [¹¹¹In]**46** tumor uptake. A group of CC49-TCO pretreated mice were injected exclusively with [¹¹¹In]**46** (without blocking) and the determined uptake was

used as reference value (100%) to normalize the observed changes in tumor uptake in blocking experiments.

Figure 2A displays the blocking assay and 2B summarizes the results for the entire Tz-library in the assay. The highest blocking efficiencies (95–99%) were observed for the Tz-chelator conjugates **4**, **24**, **35** and **41**, the Tz-carboxylic acids **33** and **39**, the Tz-PEG derivative **40**, and the Tz-sugar conjugate **45**. All of these probes include H-phenyl-, pyrimidyl-phenyl-, or *bis*(pyridyl)-Tz-scaffolds with second-order rate constants for the reaction with TCO (1,4-dioxane, 25 °C) of >70 M^{-1} s^{-1} (cf. Table 1). Further details of the blocking studies are provided in the Supporting Information (Figure S2). Next, potential correlations between the blocking effect, the clog$D_{7.4}$ and the TPSA, as well as IEDDA reactivity were investigated. As expected, high IEDDA reactivity was shown to directly correlate with the blocking effect and thus confirmed to be a key parameter for the *in vivo* ligation performance of Tz derivatives (Fig. 2C, 2D). We did not observe a strong correlation between the blocking effect and TPSA (Figure S14). However, a distinct relationship between clog$D_{7.4}$ values and the blocking effect was evidently observed when comparing Tz-derivatives with similar IEDDA reactivity (Fig. 2C, 2D and S15). For all Tz-scaffolds a Pearson's correlation coefficient >0.78 was found. Our results show that high IEDDA reactivity (> 50,000 M^{-1} s^{-1}) and a clog$D_{7.4}$ of -3 or lower are strong indicators for high *in vivo* ligation performance of Tz-derivatives in pretargeting approaches using the described tumor model (Figure 2).
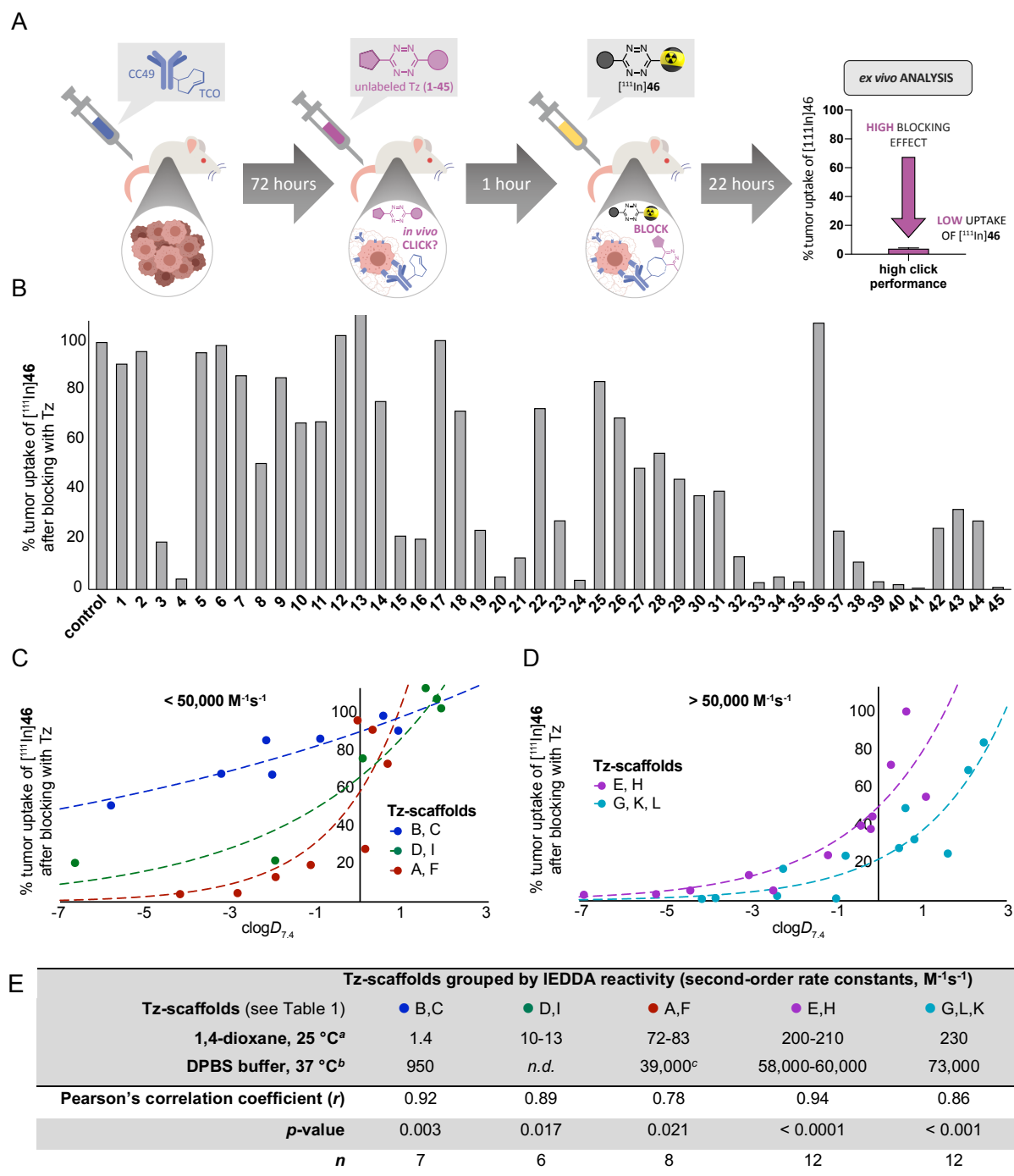
Figure 2. Results from the blocking assay. (**A**) Schematic display of the blocking assay. (**B**) The blocking effect of non-radiolabeled Tz was determined as the change in tumor uptake of [^{111}In]**46** 22 h p.i. Each Tz was administered 1 h prior to [^{111}In]**46** and the uptake normalized to a group of animals were no blocking was performed (control). Data represent mean from n = 3 mice/group, detailed information can be found in the SI. (**C** and **D**) Correlation of blocking effect and clog$D_{7.4}$ for Tz-derivatives with similar IEDDA reactivity. Data was fitted to exponential growth equation Y= Y$_0$ e^{kx} (dotted line). (**E**) Statistical analysis of the correlation between tumor uptake and clog$D_{7.4}$ for the different groups of Tz-derivatives. Pearson's correlation coefficient (r) describes the goodness of fit between the blocking effect and clog$D_{7.4}$. Notes: [a] Reaction of representative Tz with unsubstituted TCO; [b] Reaction of representative Tz with TCO-PEG$_4$; [c] Measured for Tz-scaffold A only; $n.d.$ = not determined.

Experimental design of a [^{18}F]Tz library

In order to verify that the results from the blocking study can be used to predict the outcome for *in vivo* PET imaging, 18 Tz-derivatives from the first library were selected. The selection was based on criteria such as, the possibility for ^{18}F-labeling, structural diversity,

lipophilicities and distinct IEDDA reactivities. For this purpose, we decided to use an indirect radiolabeling approach, enabling the combination of different building blocks to rapidly access a series of ^{18}F-labeled Tz-derivatives. The Cu-catalyzed azide-alkyne [3+2] cycloaddition (CuAAC) appeared to be suitable in this respect, as it allows for fast and efficient radiolabeling under mild reaction conditions.[28-32] Six precursor Tz-alkynes (**I–VI**) were prepared and reacted with three ^{18}F-labeled azides ([^{18}F]**Az1**–**Az3**) to obtain 18 different [^{18}F]Tz-probes (Table 2).

Indirect ^{18}F-labeling of a Tz series via Cu-catalyzed click chemistry

Azide building blocks were ^{18}F-labeled using fully automated procedures to afford [^{18}F]**Az1**–[^{18}F]**Az3** (Scheme S15)[33,34] and Tz-alkynes **I–VI** were synthesized as described in the Supporting Information. Subsequent radiolabeling via the CuAAC was achieved in various yields, up to approximately 70% (Table 2). Applied conditions for the CuAAC differed depending on the substituents attached to the Tz-scaffold. In general, radiolabeling was carried out at room temperature with reaction times of 10–15 min using aqueous solutions of $CuSO_4$, sodium ascorbate and disodium bathophenanthroline disulfonate (BPDS). For the synthesis of the *bis*(pyridyl)Tz-derivatives [^{18}F]**25**, [^{18}F]**44** and [^{18}F]**45**, increased amounts of the catalysts, longer reaction times (20–25 min) and elevated temperatures (120 °C) were required in order to reach radiochemical conversions (RCCs) of $\geq$ 70%. A possible reason for the harsher conditions required for this scaffold may be a result from coordination of Cu by the *bis*(pyridyl)-Tz moiety. Radiochemical yields (RCYs) and molar activities (A_m) for all ^{18}F-labeled Tz-derivatives are presented in Table 2. Radiochemical purities (RCPs) of the isolated compounds were high (> 90%), except for [^{18}F]**25** and [^{18}F]**26** (83–85%) due to radiolysis (observed for [^{18}F]**25**), undesired decomposition, and difficult separation of the resulting byproducts. During the radiolabeling partial reduction of [^{18}F]**19** and [^{18}F]**44** to the corresponding dihydro-Tz (cf. Fig. S73 and S74) was observed. However, these Tz-derivatives were reoxidized using phenyliodonium diacetate (PIDA). In the case of [^{18}F]**44**, complete reduction to the dihydro-Tz (using ascorbic acid) and reoxidation upon purification could be applied to prevent radiolysis. Excess PIDA and byproducts were removed during solid-phase extraction to obtain [^{18}F]**44** in a RCP of 98% (Table 2; for details see the Supporting Information). Moreover, during the synthesis of [^{18}F]**45** an alternative deprotection method for the azide ([^{18}F]**Az3**) was required to avoid decomposition of the Tz-scaffold during the CuAAC. All ^{18}F-labeled Tz-derivatives were formulated in 0.9% saline

prior further studies. Overall, radiofluorination via the CuAAC allowed for the preparation of a structurally diverse series of ^{18}F-labeled Tz-derivatives. In contrast to routinely used direct radiofluorination methods, this building block approach gave access to highly reactive [^{18}F]Tz-probes, using Tz-scaffolds that have previously been reported to be inaccessible.[1,35,36]
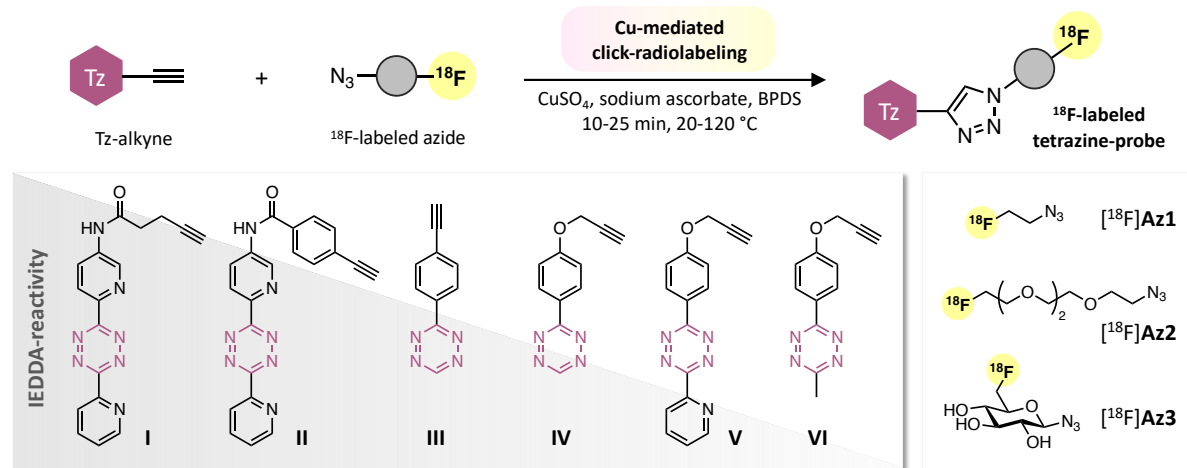

Table 2. Cu-mediated click-radiolabeling for the synthesis of ^{18}F-labeled Tz-probes.

Tetrazine	Tz-alkyne (I-VI)	Azide-functionalized ^{18}F-click-agent	RCY (%)[a]	A_m[b] (GBq/µmol)	RCP (%)[c]	*In vivo* stability[d] (% intact [^{18}F]Tz after 30 min)	Blocking effect (%) (of unlabeled Tz)
[^{18}F]1	IV	[^{18}F]Az1	25[c]	55	99	90	9
[^{18}F]2	IV	[^{18}F]Az2	23	22	96	37	4
[^{18}F]3	IV	[^{18}F]Az3	61	31	98	76	81
[^{18}F]5	VI	[^{18}F]Az1	14*	106	≥99	26	10
[^{18}F]6	VI	[^{18}F]Az2	33	100	≥99	85	1
[^{18}F]7	VI	[^{18}F]Az3	52	230	≥99	60	3
[^{18}F]12	V	[^{18}F]Az1	1*	107	96	10	0
[^{18}F]13	V	[^{18}F]Az2	11	21	94	16	0
[^{18}F]14	V	[^{18}F]Az3	68	102	98	43	24
[^{18}F]17	III	[^{18}F]Az1	8*	209	98	32	0
[^{18}F]18	III	[^{18}F]Az2	17	37	92	22	29
[^{18}F]19	III	[^{18}F]Az3	59	29	98	87	76
[^{18}F]25	II	[^{18}F]Az1	16*	n.d.	83	n.d.	16
[^{18}F]26	II	[^{18}F]Az2	36	54	≥85	27	30
[^{18}F]27	II	[^{18}F]Az3	18*	n.d.	≥90	n.d.	51
[^{18}F]43	I	[^{18}F]Az1	1	5	90	10	67
[^{18}F]44	I	[^{18}F]Az2	20	85	98	n.d.	72
[^{18}F]45	I	[^{18}F]Az3	11	151	≥90	42	99

Notes: Details on experimental procedures are provided in the Supporting Information. [a]RCYs were decay-corrected to the starting amount of radioactivity for the respective azide or *RCY was determined starting from [18]F-. [b]Molar activities (A_m) differ due to the use of different cyclotrons (see Supporting Information). [c]RCP was determined by radio-HPLC. [d]*In vivo* stability of [^{18}F]Tz was assessed by determining the fraction (%) of radioactivity corresponding to intact compound after 30 min ($n = 4$) from radio-TLC analysis. n.d. = not determined.

In vivo stability of ^{18}F-labeled Tz-derivatives in naïve mice

Next, we investigated whether there is a relationship between the *in vivo* stability of Tz-derivatives and their blocking ability. Fifteen ^{18}F-labeled tetrazines were studied in naïve

mice and collected plasma samples were analyzed by radio-TLC (for details see Supporting Information) for stability assessment (Table 2, Figure S75 and S76). Interestingly, the *in vivo* stability had only a limited or even no effect on the *in vivo* ligation performance as evaluated in the blocking study (cf. Table 1). Consequently, six [^{18}F]Tz ([^{18}F]**1**, [^{18}F]**3**, [^{18}F]**19**, [^{18}F]**26**, [^{18}F]**44**, and [^{18}F]**45**) were selected for further *in vivo* studies solely based on the IEDDA-reactivity (second-order rate constants between 72 and 230 M^{-1}s^{-1}) and lipophilicity (clog$D_{7.4}$ between -1.53 and 2.10). These radiolabeled Tz-probes were used to investigate if the results from the blocking assay can be translated to pretargeted PET imaging at tracer doses.

Pretargeted PET imaging

Of the six Tz-probes selected for evaluation in pretargeted PET imaging studies, four compounds (**3, 19, 44** and **45**) showed a good to excellent blocking effect (72–99%), while two probes (**1** and **26**) only showed limited effect (9% for **1** and 30% for **26**). The latter were included to verify that blocking results can reliably be used to predict the capability of radiolabeled Tz for pretargeted *in vivo* chemistry.

Mice (*n* = 3–4 per group) were injected *i.v.* with either CC49-TCO or 0.9% saline (control experiments). After 72 h, ^{18}F-labeled Tz (5–10 MBq) were administered and the mice were PET/CT-scanned 1 h p.i. A 3D region of interest (ROI) was created on the entire tumor volume, as well as heart and muscle tissue, and the uptake was quantified as percentage of the injected dose per gram (mean % ID/g), tumor-to-blood (T/B) and tumor-to-muscle (T/M) ratios (Fig. 3A-D, Table S3 and S4).

The tumor uptake of the different ^{18}F-labeled Tz-probes was at a rather similar level, however, [^{18}F]**3**, [^{18}F]**19** and [^{18}F]**45** showed a significantly increased tumor accumulation in mice pretreated with CC49-TCO compared to control animals (Figure 3A and 3F, Table S3 and S4). As expected and in accordance with blocking results, we did not observe significant tumor uptake of [^{18}F]**1** and [^{18}F]**26**. In the case of [^{18}F]**44,** no increase in tumor accumulation was observed in mice pretreated with TCO-modified mAb. However, this Tz showed higher radioactivity levels in the heart in mice pretreated with CC49-TCO compared to controls (2.5 ± 0.7 %ID/g and 1.5 ± 0.2 %ID/g, respectively; Figure 3B, Table S1). This indicates that [^{18}F]**44** binds to mAb still circulating in the blood pool. This difference was also observed for the three ^{18}F-labeled Tz-derivatives showing specific tumor accumulation ([^{18}F]**3**, [^{18}F]**19** and [^{18}F]**45**)**,** but not for the non-accumulating probes [^{18}F]**1** and [^{18}F]**26** (Figure 3B). Binding to residual mAb in the blood pool is a frequently reported challenge in pretargeted imaging approaches, and has been addressed by the development of clearing agents.[14,37-39] However,

ligation in blood did not hinder the investigation of the *in vivo* ligation performance of ^{18}F-labeled Tz-probes in comparison to blocking efficiencies.

Finally, the relationship between the *in vivo* performance of the used Tz-probes and the results obtained from the blocking assay was investigated. A strong correlation was found between the blocking effect of the unlabeled Tz and the T/M ratio (Figure 3D) as well as the selective tumor uptake (tumor to tumor-control (T/Tc) ratio) (Figure S78 and Table S4) of the respective ^{18}F-labeled probes in pretargeted PET imaging studies. These significant relationships confirm the validity of the blocking assay and our finding that reduced lipophilicity and high IEDDA reactivity are key parameters for the *in vivo* performance of Tz-derivatives. Our results show that low lipophilicity enhances the ability of the bioorthogonal Tz-agent to bind to TCO-mAbs at the tumor site. Moreover, faster excretion of radiolabeled probes, which is crucial for obtaining high tumor-to-background ratios is also facilitated by low lipophilicity of Tz-derivatives (Figure 3).
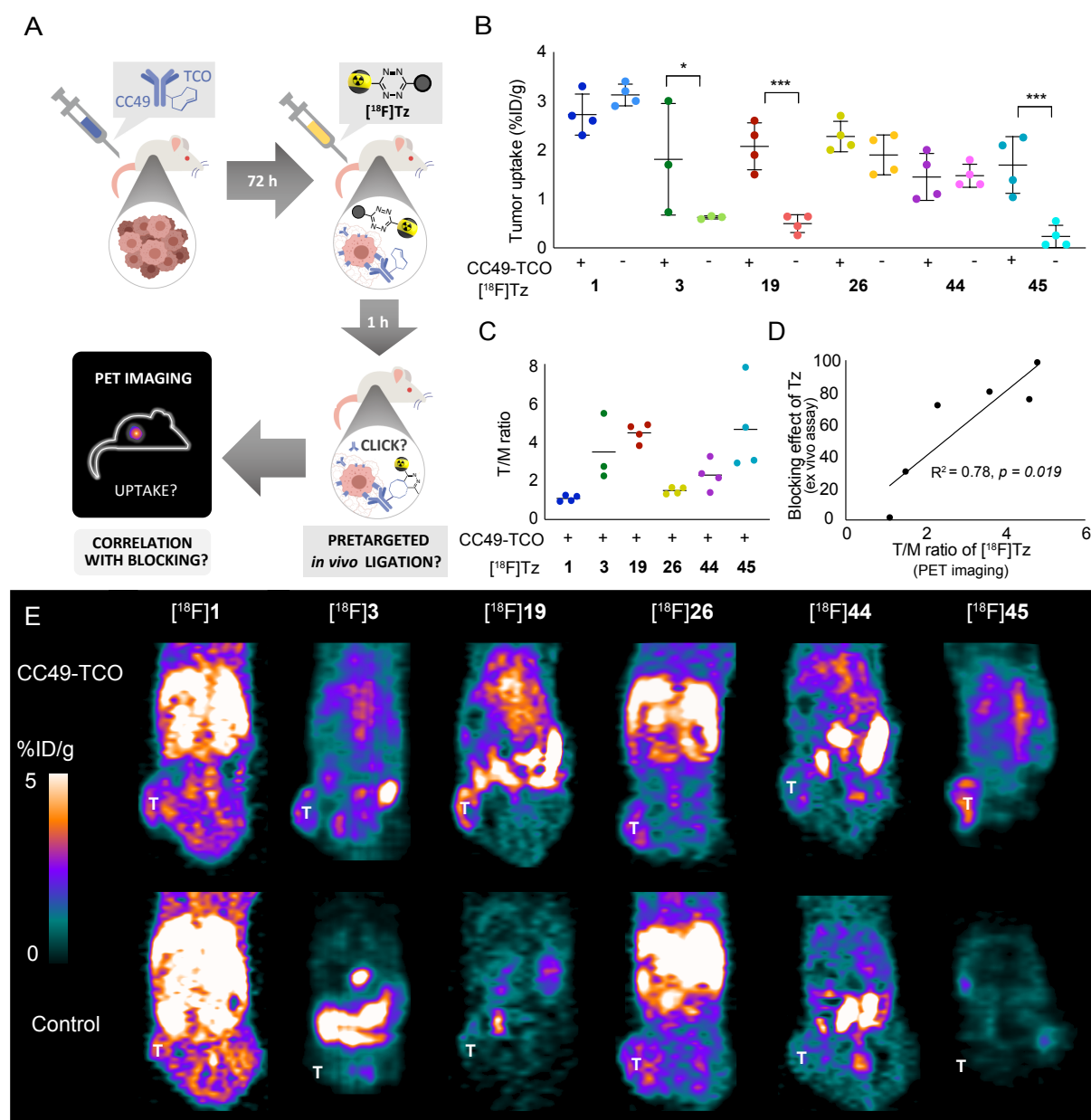
Figure 3. Pretargeted PET imaging in BALB/c nude mice bearing LS174T tumor xenografts with six ^{18}F-labeled Tz-derivatives. Animals were treated with CC49-TCO or saline (control) 72 h prior to injection of the radiolabeled Tz-derivative. (**A**) Schematic illustration of the pretargeting experiment and the research question: Is there a correlation between the blocking effect and the PET imaging contras. (**B**) Image-derived mean uptake values are presented as percentage of the injected dose per gram (%ID/g) in tumor. (**C**) Tumor-to-muscle (T/M) ratios ($n = 4$ mice, except for [^{18}F]**3**, $n = 3$). Data is represented as mean ± S.D. (*$p < 0.05$ and ***$p < 0.001$). For all groups $n = 4$ mice (except [^{18}F]**3** where $n = 3$) (**D**) Correlation between the blocking effect of the unlabeled Tz-derivatives **1**, **3**, **19**, **26**, **44**, and **45** and the T/M-ratios for the corresponding ^{18}F-labeled compounds observed by *in vivo* pretargeted PET imaging. A strong correlation was found (linear regression: $R^2 = 0.78$, $p = 0.019$, $n = 6$). Data is represented as mean ± S. D. The asterisk indicates significant difference (* $p < 0.05$ and *** $p < 0.001$) when compared to control. (**E**) Representative images of PET scans 1 h p.i. of the radiolabeled Tz ([^{18}F]**1**, [^{18}F]**3**, [^{18}F]**19**, [^{18}F]**26**, [^{18}F]**44** and [^{18}F]**45**) in pretargeted PET imaging studies (T indicates the position of the tumor). [^{18}F]**3**, [^{18}F]**19** and [^{18}F]**45** displayed specific tumor uptake and the tumor is clearly visualized in the PET image.

CONCLUSION

The advancement of *in vivo* chemical tools based on a better understanding of the scope and limitations of bioorthogonal reactions, *in vitro* and in living systems, paves the way to clinical translation of pretargeting approaches for diagnostic (*e.g.* pretargeted imaging

[29,36,38,40-46]) and therapeutic application (e.g. pretargeted radionuclide therapy[1,16,19,20,47] or bioorthogonal cleavage of antibody-drug conjugates[2,17,18]). However, progress in this field is limited due to the required elaborate development of (radio)labeled compounds for *in vivo* evaluation, hampering the use of compound libraries for systematic studies to gain further insight. The developed blocking assay described herein tackles this challenge. By screening of 45 unlabeled Tz-derivatives, we were able to reveal the key parameters that are necessary for a Tz to be applied in pretargeting. High IEDDA-reactivity of the Tz-scaffold with a second-order rate constant of $>50,000$ $M^{-1}s^{-1}$ was shown to be an important parameter to achieve efficient *in vivo* ligation ($>96\%$ blocking) to pretargeted mAb-TCO conjugates in LS174T xenografts. Unexpectedly, reduced lipophilicity was identified to play an even more decisive role, with $clogD_{7.4}$ values being a strong indicator for the *in vivo* ligation performance of Tz-derivatives. In particular, $clogD_{7.4}$ values below -3 increased the chances for successful *in vivo* ligation in the applied tumor model. These key findings from the blocking study were confirmed by pretargeted PET imaging. The increasing knowledge regarding the IEDDA-reactivity of various Tz-scaffolds, as well as the fact that calculated parameters (*i.e.* $clogD_{7.4}$) can be used may guide and accelerate the design and development of Tz-derivatives for *in vivo* applications.

Overall, we present and demonstrate a new strategy and method for the systematic investigation of bioorthogonal pretargeting. The concept of our blocking assay can be translated to other tumor models and/or targets, in combination with respective mAbs as targeting vectors/carriers. We believe that the revealed key parameters enable the development of Tz-derivatives as multifunctional tools for diagnostic and therapeutic applications, ultimately to improve and accelerate the clinical translation of *in vivo* chemistry.

ASSOCIATED CONTENT

Supporting Information

Details on experimental procedures for organic synthesis, radiochemistry, reaction kinetics and *in vivo* studies are provided in the Supporting Information. All animal experiments in this study were approved by national animal welfare committees in Austria and Denmark, and the experiments were performed in accordance with European guidelines.

AUTHOR INFORMATION

Corresponding Author

*Matthias M. Herth

Department of Drug Design and Pharmacology, University of Copenhagen

Jagtvej 160, 2100 Copenhagen Ø, Denmark

Tel: +45 3533 6624

E-mail: matthias.herth@sund.ku.dk

*Andreas Kjaer

Department of Clinical Physiology, Nuclear Medicine & PET, Rigshospitalet

Blegdamsvej 9, 2100 Copenhagen Ø, Denmark

Tel: +45 2725 8614

E-mail: akjaer@sund.ku.dk

*Hannes Mikula

Institute of Applied Synthetic Chemistry, TU Wien

Getreidemarkt 9, 1060 Vienna, Austria

orcid.org/0000-0002-9218- 9722

E-mail: hannes.mikula@tuwien.ac.at

Author Contributions

[T] EJLS, JTJ and CD contributed equally to the work. The experimental work was carried out through contributions of EJLS, JTJ, CD, UMB, KN, PEE, KB, VS, MW, DS, CBMP, LH, MSM, TW and RR. The study was designed by EJLS, JTJ, CD, UMB, KN, PEE, MR, JLK, HM, AK and MMH. The manuscript was written through contributions of all authors. All authors have given approval to the final version of the manuscript.

REFERENCES

1. Steen, E. J. L.; Edem, P. E.; Norregaard, K.; Jorgensen, J. T.; Shalgunov, V.; Kjaer, A.; Herth, M. M., Pretargeting in nuclear imaging and radionuclide therapy: Improving efficacy of theranostics and nanomedicines. *Biomaterials* **2018,** *179*, 209-245.

2. Rossin, R.; Versteegen, R. M.; Wu, J.; Khasanov, A.; Wessels, H. J.; Steenbergen, E. J.; Ten Hoeve, W.; Janssen, H. M.; van Onzen, A.; Hudson, P. J.; Robillard, M. S., Chemically triggered drug release from an antibody-drug conjugate leads to potent antitumour activity in mice. *Nat. Commun.* **2018,** *9* (1), 1484.

3. Hapuarachchige, S.; Artemov, D., Theranostic Pretargeting Drug Delivery and Imaging Platforms in Cancer Precision Medicine. *Front. Oncol.* **2020,** *10*, 1131.

4. Altai, M.; Membreno, R.; Cook, B.; Tolmachev, V.; Zeglis, B. M., Pretargeted Imaging and Therapy. *J. Nucl. Med.* **2017,** *58* (10), 1553-1559.

5. Scott, A. M.; Wolchok, J. D.; Old, L. J., Antibody therapy of cancer. *Nat. Rev. Cancer.* **2012,** *12* (4), 278-87.

6. van Dongen, G. A.; Visser, G. W.; Lub-de Hooge, M. N.; de Vries, E. G.; Perk, L. R., Immuno-PET: a navigator in monoclonal antibody development and applications. *Oncologist* **2007,** *12* (12), 1379-89.

7. Boswell, C. A.; Brechbiel, M. W., Development of radioimmunotherapeutic and diagnostic antibodies: an inside-out view. *Nucl. Med. Biol.* **2007,** *34* (7), 757-78.

8. Larson, S. M.; Carrasquillo, J. A.; Cheung, N. K.; Press, O. W., Radioimmuno-therapy of human tumours. *Nat. Rev. Cancer.* **2015,** *15* (6), 347-60.

9. Borjesson, P. K.; Jauw, Y. W.; de Bree, R.; Roos, J. C.; Castelijns, J. A.; Leemans, C. R.; van Dongen, G. A.; Boellaard, R., Radiation dosimetry of [89]Zr-labeled chimeric monoclonal antibody U36 as used for immuno-PET in head and neck cancer patients. *J. Nucl. Med.* **2009,** *50* (11), 1828-36.

10. Dijkers, E. C.; Oude Munnink, T. H.; Kosterink, J. G.; Brouwers, A. H.; Jager, P. L.; de Jong, J. R.; van Dongen, G. A.; Schroder, C. P.; Lub-de Hooge, M. N.; de Vries, E. G., Biodistribution of [89]Zr-trastuzumab and PET imaging of HER2-positive

lesions in patients with metastatic breast cancer. *Clin. Pharmacol. Ther.* **2010,** *87* (5), 586-92.

11. Reardan, D. T.; Meares, C. F.; Goodwin, D. A.; McTigue, M.; David, G. S.; Stone, M. R.; Leung, J. P.; Bartholomew, R. M.; Frincke, J. M., Antibodies against metal chelates. *Nature* **1985,** *316* (6025), 265-8.

12. Goodwin, D. A.; Mears, C. F.; McTigue, M.; David, G. S., Monoclonal antibody hapten radiopharmaceutical delivery. *Nucl. Med. Commun.* **1986,** *7* (8), 569-80.

13. Rossin, R.; Verkerk, P. R.; van den Bosch, S. M.; Vulders, R. C.; Verel, I.; Lub, J.; Robillard, M. S., In vivo chemistry for pretargeted tumor imaging in live mice. *Angew. Chem. Int. Ed.* **2010,** *49* (19), 3375-8.

14. Zeglis, B. M.; Brand, C.; Abdel-Atti, D.; Carnazza, K. E.; Cook, B. E.; Carlin, S.; Reiner, T.; Lewis, J. S., Optimization of a Pretargeted Strategy for the PET Imaging of Colorectal Carcinoma via the Modulation of Radioligand Pharmacokinetics. *Mol. Pharm.* **2015,** *12* (10), 3575-87.

15. Rossin, R.; Lappchen, T.; van den Bosch, S. M.; Laforest, R.; Robillard, M. S., Diels-Alder reaction for tumor pretargeting: in vivo chemistry can boost tumor radiation dose compared with directly labeled antibody. *J. Nucl. Med.* **2013,** *54* (11), 1989-95.

16. Keinanen, O.; Fung, K.; Brennan, J. M.; Zia, N.; Harris, M.; van Dam, E.; Biggin, C.; Hedt, A.; Stoner, J.; Donnelly, P. S.; Lewis, J. S.; Zeglis, B. M., Harnessing (64)Cu/(67)Cu for a theranostic approach to pretargeted radioimmunotherapy. *Proc. Natl. Acad. Sci.* **2020,** *117* (45), 28316-27.

17. Ediriweera, G. R.; Simpson, J. D.; Fuchs, A. V.; Venkatachalam, T. K.; Van De Walle, M.; Howard, C. B.; Mahler, S. M.; Blinco, J. P.; Fletcher, N. L.; Houston, Z. H.; Bell, C. A.; Thurecht, K. J., Targeted and modular architectural polymers employing bioorthogonal chemistry for quantitative therapeutic delivery. *Chem. Sci.* **2020,** *11* (12), 3268-80.

18. Khan, I.; Agris, P. F.; Yigit, M. V.; Royzen, M., In situ activation of a doxorubicin prodrug using imaging-capable nanoparticles. *Chem. Commun.* **2016,** *52* (36), 6174-77.

19. Wilkovitsch, M.; Haider, M.; Sohr, B.; Herrmann, B.; Klubnick, J.; Weissleder, R.; Carlson, J. C. T.; Mikula, H., A Cleavable C2-Symmetric trans-Cyclooctene Enables Fast and Complete Bioorthogonal Disassembly of Molecular Probes. *J. Am. Chem. Soc.* **2020,** *142* (45), 19132-41.

20. Carlson, J. C. T.; Mikula, H.; Weissleder, R., Unraveling Tetrazine-Triggered Bioorthogonal Elimination Enables Chemical Tools for Ultrafast Release and Universal Cleavage. *J. Am. Chem. Soc.* **2018,** *140* (10), 3603-12.

21. Rossin, R.; van Duijnhoven, S. M.; Ten Hoeve, W.; Janssen, H. M.; Kleijn, L. H.; Hoeben, F. J.; Versteegen, R. M.; Robillard, M. S., Triggered Drug Release from an Antibody-Drug Conjugate Using Fast "Click-to-Release" Chemistry in Mice. *Bioconjugate Chem.* **2016,** *27* (7), 1697-706.

22. Versteegen, R. M.; Rossin, R.; ten Hoeve, W.; Janssen, H. M.; Robillard, M. S., Click to release: instantaneous doxorubicin elimination upon tetrazine ligation. *Angew Chem. Int. Ed.* **2013,** *52* (52), 14112-6.

23. Blackman, M. L.; Royzen, M.; Fox, J. M., Tetrazine ligation: Fast bioconjugation based on inverse-electron-demand Diels-Alder reactivity. *J. Am. Chem. Soc.* **2008,** *130* (41), 13518-9.

24. Darko, A.; Wallace, S.; Dmitrenko, O.; Machovina, M. M.; Mehl, R. A.; Chin, J. W.; Fox, J. M., Conformationally strained trans-cyclooctene with improved stability and excellent reactivity in tetrazine ligation. *Chem. Sci.* **2014,** *5* (10), 3770-6.

25. Evans, H. L.; Nguyen, Q. D.; Carroll, L. S.; Kaliszczak, M.; Twyman, F. J.; Spivey, A. C.; Aboagye, E. O., A bioorthogonal ^{68}Ga-labelling strategy for rapid in vivo imaging. *Chem. Commun.* **2014,** *50* (67), 9557-60.

26. Zeglis, B. M.; Sevak, K. K.; Reiner, T.; Mohindra, P.; Carlin, S. D.; Zanzonico, P.; Weissleder, R.; Lewis, J. S., A Pretargeted PET Imaging Strategy Based on Bioorthogonal Diels-Alder Click Chemistry. *J.Nuc.Med.* **2013,** *54* (8), 1389-96.

27. Rossin, R.; van den Bosch, S. M.; Ten Hoeve, W.; Carvelli, M.; Versteegen, R. M.; Lub, J.; Robillard, M. S., Highly reactive trans-cyclooctene tags with improved stability for Diels-Alder chemistry in living systems. *Bioconjugate Chem.* **2013,** *24* (7), 1210-7.

28. Gill, H. S.; Marik, J., Preparation of ^{18}F-labeled peptides using the copper(I)-catalyzed azide-alkyne 1,3-dipolar cycloaddition. *Nat. Protoc.* **2011,** *6* (11), 1718-25.

29. Meyer, J. P.; Adumeau, P.; Lewis, J. S.; Zeglis, B. M., Click Chemistry and Radiochemistry: The First 10 Years. *Bioconjugate Chem.* **2016,** *27* (12), 2791-807.

30. Ross, T. L.; Honer, M.; Lam, P. Y. H.; Mindt, T. L.; Groehn, V.; Schibli, R.; Schubiger, P. A.; Ametamey, S. M., Fluorine-18 Click Radiosynthesis and Preclinical Evaluation of a New ^{18}F-Labeled Folic Acid Derivative. *Bioconjugate Chem.* **2008,** *19* (12), 2462-70.

31. Marik, J.; Sutcliffe, J. L., Click for PET: rapid preparation of [^{18}F]fluoropeptides using Cu-I catalyzed 1,3-dipolar cycloaddition. *Tetrahedron Lett.* **2006,** *47* (37), 6681-4.

32. Glaser, M.; Arstad, E., "Click labeling" with 2-[^{18}F]fluoroethylazide for positron emission tomography. *Bioconjugate Chem.* **2007,** *18* (3), 989-93.

33. Denk, C.; Wilkovitsch, M.; Skrinjar, P.; Svatunek, D.; Mairinger, S.; Kuntner, C.; Filip, T.; Frohlich, J.; Wanek, T.; Mikula, H., [^{18}F]Fluoroalkyl azides for rapid radiolabeling and (Re)investigation of their potential towards in vivo click chemistry. *Org. Biomol. Chem.* **2017,** *15* (28), 5976-82.

34. Maschauer, S.; Haubner, R.; Kuwert, T.; Prante, O., ^{18}F-glyco-RGD peptides for PET imaging of integrin expression: efficient radiosynthesis by click chemistry and modulation of biodistribution by glycosylation. *Mol. Pharm.* **2014,** *11* (2), 505-15.

35. Li, Z.; Cai, H.; Hassink, M.; Blackman, M. L.; Brown, R. C.; Conti, P. S.; Fox, J. M., Tetrazine-trans-cyclooctene ligation for the rapid construction of ^{18}F-labeled probes. *Chem. Commun.* **2010,** *46* (42), 8043-5.

36. Denk, C.; Svatunek, D.; Filip, T.; Wanek, T.; Lumpi, D.; Frohlich, J.; Kuntner, C.; Mikula, H., Development of a ^{18}F-labeled tetrazine with favorable pharmacokinetics for bioorthogonal PET imaging. *Angew. Chem. Int. Ed.* **2014,** *53* (36), 9655-9.

37. Steen, E. J. L.; Jorgensen, J. T.; Johann, K.; Norregaard, K.; Sohr, B.; Svatunek, D.; Birke, A.; Shalgunov, V.; Edem, P. E.; Rossin, R.; Seidl, C.; Schmid, F.; Robillard, M. S.; Kristensen, J. L.; Mikula, H.; Barz, M.; Kjaer, A.; Herth, M. M., Trans-Cyclooctene-Functionalized PeptoBrushes with Improved Reaction Kinetics of the Tetrazine Ligation for Pretargeted Nuclear Imaging. *ACS Nano* **2020,** *14* (1), 568-84.

38. Meyer, J. P.; Kozlowski, P.; Jackson, J.; Cunanan, K. M.; Adumeau, P.; Dilling, T. R.; Zeglis, B. M.; Lewis, J. S., Exploring Structural Parameters for Pretargeting Radioligand Optimization. *J. Med. Chem.* **2017,** *60* (19), 8201-17.

39. Keinanen, O.; Fung, K.; Pourat, J.; Jallinoja, V.; Vivier, D.; Pillarsetty, N. K.; Airaksinen, A. J.; Lewis, J. S.; Zeglis, B. M.; Sarparanta, M., Pretargeting of internalizing trastuzumab and cetuximab with a ^{18}F-tetrazine tracer in xenograft models. *EJNMMI Res.* **2017,** *7* (1), 95.

40. Denk, C.; Svatunek, D.; Mairinger, S.; Stanek, J.; Filip, T.; Matscheko, D.; Kuntner, C.; Wanek, T.; Mikula, H., Design, Synthesis, and Evaluation of a Low-

Molecular-Weight ^{11}C-Labeled Tetrazine for Pretargeted PET Imaging Applying Bioorthogonal in Vivo Click Chemistry. *Bioconjugate Chem.* **2016,** *27* (7), 1707-12.

41.   Edem, P. E.; Jorgensen, J. T.; Norregaard, K.; Rossin, R.; Yazdani, A.; Valliant, J. F.; Robillard, M.; Herth, M. M.; Kjaer, A., Evaluation of a ^{68}Ga-Labeled DOTA-Tetrazine as a PET Alternative to ^{111}In-SPECT Pretargeted Imaging. *Molecules* **2020,** *25* (3).

42.   Steen, E. J. L.; Jorgensen, J. T.; Petersen, I. N.; Norregaard, K.; Lehel, S.; Shalgunov, V.; Birke, A.; Edem, P. E.; L'Estrade, E. T.; Hansen, H. D.; Villadsen, J.; Erlandsson, M.; Ohlsson, T.; Yazdani, A.; Valliant, J. F.; Kristensen, J. L.; Barz, M.; Knudsen, G. M.; Kjaer, A.; Herth, M. M., Improved radiosynthesis and preliminary in vivo evaluation of the ^{11}C-labeled tetrazine [^{11}C]AE-1 for pretargeted PET imaging. *Bioorg. Med. Chem. Lett.* **2019,** *29* (8), 986-90.

43.   Meyer, J. P.; Houghton, J. L.; Kozlowski, P.; Abdel-Atti, D.; Reiner, T.; Pillarsetty, N. V. K.; Scholz, W. W.; Zeglis, B. M.; Lewis, J. S., ^{18}F-Based Pretargeted PET Imaging Based on Bioorthogonal Diels Alder Click Chemistry. *Bioconjugate Chem.* **2016,** *27* (2), 298-301.

44.   Edem, P. E.; Sinnes, J. P.; Pektor, S.; Bausbacher, N.; Rossin, R.; Yazdani, A.; Miederer, M.; Kjaer, A.; Valliant, J. F.; Robillard, M. S.; Rosch, F.; Herth, M. M., Evaluation of the inverse electron demand Diels-Alder reaction in rats using a [44]Sc-labelled tetrazine for pretargeted PET imaging. *EJNMMI Res.* **2019,** *9*.

45.   Keinanen, O.; Li, X. G.; Chenna, N. K.; Lumen, D.; Ott, J.; Molthoff, C. F.; Sarparanta, M.; Helariutta, K.; Vuorinen, T.; Windhorst, A. D.; Airaksinen, A. J., A New Highly Reactive and Low Lipophilicity Fluorine-18 Labeled Tetrazine Derivative for Pretargeted PET Imaging. *ACS. Med. Chem. Lett.* **2016,** *7* (1), 62-6.

46.   Herth, M. M.; Andersen, V. L.; Lehel, S.; Madsen, J.; Knudsen, G. M.; Kristensen, J. L., Development of a ^{11}C-labeled tetrazine for rapid tetrazine-trans-cyclooctene ligation. *Chem. Commun.* **2013,** *49* (36), 3805-7.

47.   Lappchen, T.; Rossin, R.; van Mourik, T. R.; Gruntz, G.; Hoeben, F. J. M.; Versteegen, R. M.; Janssen, H. M.; Lub, J.; Robillard, M. S., DOTA-tetrazine probes with modified linkers for tumor pretargeting. *Nucl. Med. Biol.* **2017,** *55*, 19-26.